ELSEVIER

Thermochimica Acta 330 (1999) 189–200

thermochimica acta

Isothermal curing of an epoxy resin by alternating differential scanning calorimetry

S. Montserrat*, I. Cima

Departament de Màquines i Motors Tèrmics, Universitat Politècnica de Catalunya, Carrer de Colom 11, E-08222 Terrassa, Spain

Received 18 September 1998; accepted 4 January 1999

Abstract

The quasi-isothermal curing of a diepoxide resin with a triamine of polyoxypropylene was studied by alternating differential scanning calorimetry (ADSC), which is a temperature modulated DSC technique. The complex heat capacity measurements allows to analyse the vitrification process at curing temperatures (T_c) below the maximum glass transition of the fully cured epoxy ($T_{g_\infty} = 85.8°C$). Initially, the modulus of the complex heat capacity, $|C_p^*|$, increases until a maximum (conversion between 0.42 and 0.56) and then decreases. This step is followed by an abrupt decay of $|C_p^*|$, due to the vitrification of the system, which allows the determination of the vitrification time. This value agrees well with that determined by the partial curing method. The phase angle and out-of-phase heat capacity show an asymmetric wide peak during the vitrification process. The change in $|C_p^*|$ at vitrification decreases with the increase of T_c becoming zero at temperature T_{g_∞}. This epoxy-triamine system shows a delay of the vitrification process respect to other model epoxy systems probably due to the presence of polyoxypropylene chains in the network.

The decay of $|C_p^*|$ during vitrification may be normalised between unity and zero by defining a mobility factor. This mobility factor has been used to simulate the reaction rate during the stage where the reaction is controlled by diffusion. The observed reaction rate is simulated by the product of the kinetic reaction rate, determined by the autocatalytic model, and the mobility factor. © 1999 Elsevier Science B.V. All rights reserved.

Keywords: Isothermal curing; Temperature modulated differential scanning calorimetry (TMDSC); Vitrification process; Epoxy resins

1. Introduction

During the isothermal cure of an epoxy resin the system changes from a viscous liquid to a highly crosslinked network. Because the reaction occurs in a condensed phase, the rate of the cure reaction is controlled by the activity of the functional groups and additionally by their mobility. During the first stages of the reaction, when the rate of displacement of the groups is much faster than the rate of molecular collisions, the reaction is controlled by the chemical reactivity of these groups. As the reaction proceeds, there is an increase in chain branching until the system reaches gelation; further polymerisation causes an increase of the crosslinking until the mobility of the reactive centres is progressively restricted and the reaction becomes diffusion controlled. This is the factor which limits the degree of conversion at curing temperatures, T_c, below the maximum glass transition of the fully cured epoxy T_{g_∞}. As the crosslinking

---

*Corresponding author. Tel.: +34-93-7398123; fax: +34-93-7398101; e-mail: montserrat@mmt.upc.es

PII: S0040-6031(99)00033-7

degree progresses T_g of the epoxy increases until it equals T_c, at which point the system reaches the glassy state and vitrifies. In these conditions the kinetics slow down and the extent of conversion tends to a practically constant limiting value [1–4].

The enthalpy and the volume of the system are expected to decrease continuously during the curing until the vitrification process. It is also expected that the heat capacity would decrease on vitrification. This change in the heat capacity has been observed by Cassettari et al. [5] during the isothermal curing of an epoxy resin using a specially designed differential microcalorimeter, where the heat flow was perturbed periodically by a heat pulse. More recently, Van Mele and co-workers [6,7] have studied the vitrification process in isothermal and non-isothermal curing of thermosetting systems by modulated differential scanning calorimetry (MDSC).

The objective of the present work is the use of alternating differential scanning calorimetry (ADSC), which is a temperature modulated DSC technique (TMDSC), to study the quasi-isothermal curing of an epoxy-triamine system at temperatures below and above the maximum glass transition $T_{g\infty}$ of the system. In particular, the vitrification process has been analysed by the heat capacity measurements. The curing kinetics during the chemical controlled reaction has been studied by the heat flow data and the diffusion controlled stage has been analysed by heat capacity measurements.

2. Alternating differential scanning calorimetry

ADSC is based on the temperature modulation during a constant heating rate, which idea was initially proposed by Reading [8–10]. In the non-isothermal experiments, the temperature T is programmed as a sinusoidal modulation of amplitude A_T and frequency ω (radian s^{-1}):

$$T = T_0 + q_0 t + A_T \sin(\omega t), \tag{1}$$

where T_0 is the initial temperature and q_0 is the underlying heating rate which is zero in isothermal experiments. Then the dependence of the heating rate on time is

$$q = q_0 + A_T \omega \cos(\omega t), \tag{2}$$

or in isothermal experiments,

$$q = A_T \omega \cos(\omega t). \tag{3}$$

As a consequence of the periodical variation of q, a periodic heat flow signal is obtained, which is shifted by a phase angle δ with respect to the heating rate. The Fourier transformation of the cycles of the heating rate and the heat flow gives the following quantities: q_0=underlying heating rate, $\langle \mathrm{HF} \rangle$=average or total heat flow, A_T=amplitude of the temperature modulation, A_{HF}=amplitude of the heating flow modulation, δ=phase angle between heat flow and heating rate.

The average value of heat flow is practically the same signal that would be obtained by conventional DSC. The ratio of this quantity and q_0 defines an average heat capacity which corresponds to that obtained by conventional DSC [11,12]. During isothermal curing, the ADSC curve of heat flow allows one to determine the heat of curing evolved during the reaction.

Adopting the approach suggested by Schawe [13] based on the linear response theory, a complex heat capacity may be defined:

$$C_p^* = C_p' - \mathrm{i} C_P'', \tag{4}$$

where C_p' is the real (in-phase) component, and C_p'' the imaginary (out-of-phase) component. The modulus of C_p^* is

$$|C_p^*| = \frac{A_{HF}}{A_q}, \tag{5}$$

where A_q is the amplitude of the heating rate modulation (A_q= $A_T\omega$).The real and imaginary heat capacities are defined as follows:

$$C_p' = |C_p^*| \cos\delta, \tag{6}$$

$$C_p'' = |C_p^*| \sin\delta. \tag{7}$$

The values of the total heat flow, heat capacities ($|C_p^*|$, C_p', and C_p'') and the phase angle have been analysed during the quasi-isothermal curing of an epoxy resin cured by a triamine at different T_c.

Alternatively, the approach of reversing and non-reversing heat flow [8–10] defines the reversing heat flow as $|C_p^*| \cdot q_0$ and the non-reversing heat flow as the differences between the total heat flow, $\langle \mathrm{HF} \rangle$, and the reversing heat flow, $\langle \mathrm{HF} \rangle_{\mathrm{Rev}}$.

$$\mathrm{HF}_{\mathrm{Non-Rev}} = \langle \mathrm{HF} \rangle - \langle \mathrm{HF} \rangle_{\mathrm{Rev}}. \tag{8}$$

For isothermal experiments, the curve of the total heat flow is the same as the non-reversing heat flow because the reversing heat flow is zero (q_0=0).

3. Experimental

The resin used was a commercial epoxy based on diglycidyl ether of bisphenol A (CIBA-GEIGY Araldite F), with an epoxy equivalent of 188.3 g/equiv cured by a triamine of polyoxypropylene (Jeffamine T-430 from Huntsman Corporation) at the stoichiometric ratio. The corresponding chemical structures are shown in Fig. 1.

The TMDSC measurements were performed by a METTLER TOLEDO 821e with an intracooler, using the software Alternating DSC (ADSC). The temperature calibration and the determination of the constant time of the instruments were performed by standards of In and Zn, and the heat flow calibration by In.

The modulation conditions used in the curing reaction were an amplitude of 0.5 K and a period of 1 min. In order to calibrate the heat flow signal, a blank with an empty pan on the reference side and an empty pan plus a lid in the sample side was performed before the sample measurement. Standard aluminium pans were used and the sample mass was about 10 mg. The experiments of quasi-isothermal curing of the resin were performed at temperatures below and above the glass transition, from 50°C to 110°C, for periods of time between 6 and 20 h depending on T_c.

The dynamic glass transition temperature of the fully cured epoxy resin was obtained by ADSC using the same conditions of modulation, 0.5 K and 1 min, and an underlying heating rate of 1 K min^{-1}.

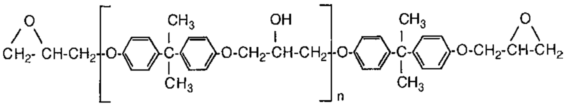

Diglycidyl ether of bisphenol A (n=0.13) (Araldite F)

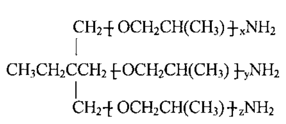

Polyoxypropylenetriamine (x+y+z≈5.3) (Jeffamine T-403)

Fig. 1. Chemical structure of the epoxy resin and the hardener.

Conventional DSC measurements were performed by a Mettler TA 4000 DSC 30, previously calibrated with metallic standards. DSC analysis of samples cured at different times and the same temperature T_c was performed to obtain the conversion degree and the corresponding T_g of the system in order to determine the vitrification conditions [14].

4. Results and discussion

4.1. Glass transition of the fully cured epoxy

Fig. 2 shows the traces of heat capacities ($|C_p^*|$, C_p' and C_p''), phase angle and heat flow (total, reversing and non-reversing) for the fully cured epoxy obtained at an underlying heating rate of 1 K min^{-1} and a modulation of 0.5 K and 1 min. The dynamic glass transition has been determined at the midpoint of the variation in the modulus of the complex heat capacity, $|C_p^*|$, which gives a value of 85.8°C, as Table 1 shows. This value was taken for the maximum glass transition of the fully cured epoxy, T_{g_∞}. The same value has been obtained in the reversing heat flow trace. The value obtained in the $|C_p^*|$ curve by cooling at 1 K min^{-1} is very similar to that obtained by heating (85.5°C). The total heat flow, which is equivalent to the heat flow obtained by conventional DSC gives a value of 82.3°C at 1 K min^{-1}. The midpoint glass transition obtained by conventional DSC at 10 K min^{-1} was 85.8°C. Table 1 gives also the corresponding values of the onset and endset glass transition temperatures, T_{g_0} and T_{g_e}, respectively.

4.2. Quasi-isothermal curing

The ADSC signal of the total heat flow shows an exothermic peak (Fig. 3) whose area is practically equal to that obtained by conventional DSC in the same curing conditions [6,7]. The total heat of curing obtained non-isothermally by conventional DSC was 358.7 J g^{-1}. The curing at $T_c < T_{g_\infty}$ gives lower heats of curing due to the vitrification effects.

In this diepoxide-triamine system, the modulus of the complex heat capacity follows a three step variation as is shown in Fig. 3 for the epoxy cured at 50°C and 80°C. Initially, $|C_p^*|$ increases until a maximum and then decreases slightly. This variation shows a

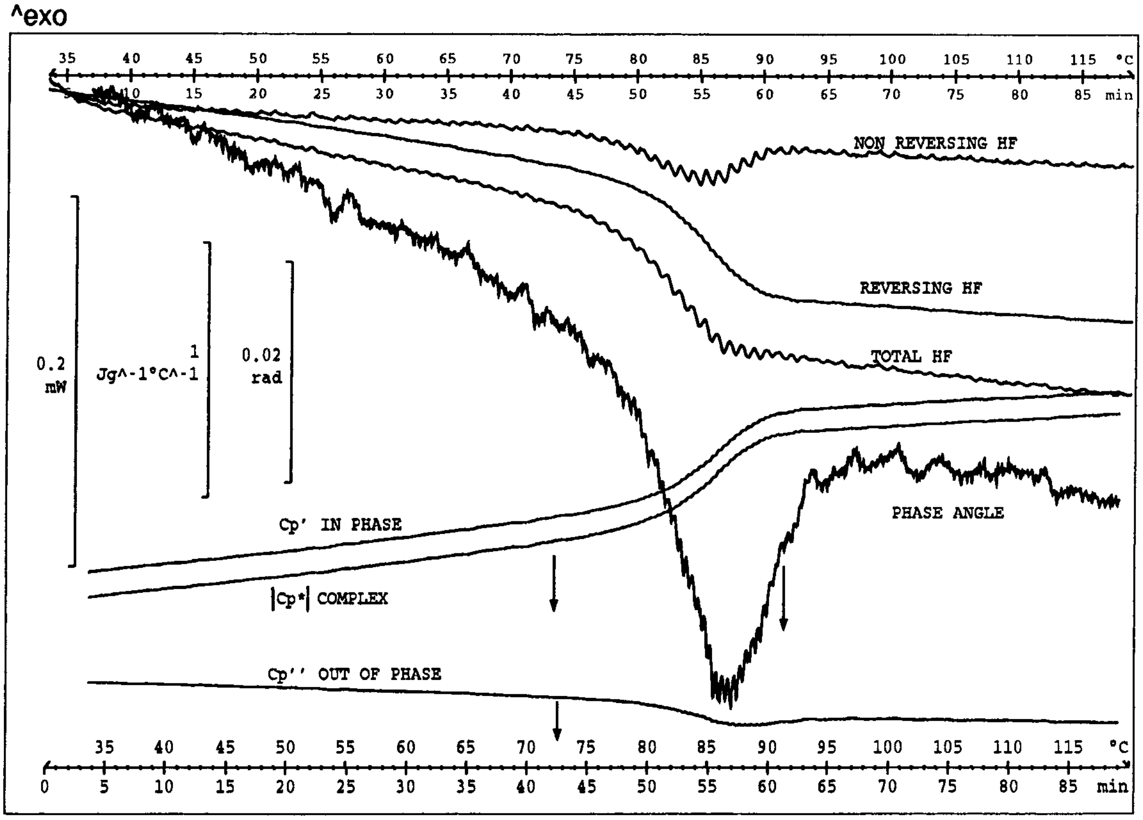

Fig. 2. ADSC curves in the glass transition region of the fully cured epoxy resin obtained at 1 K min^{-1}, 0.5 K of amplitude and 1 min of period: heat capacities ($|C_p^*|$, C_p' and C_p''), phase angle and heat flow (total, reversing and non-reversing).

broader peat at T_c=50°C which becomes sharper and shifted to lower times the higher is T_c (i.e. T_c=80°C in Fig. 3). The conversion degree at the maximum lies between 0.42 and 0.56 (Table 2). After this maximum, $|C_p^*|$ shows a slight decrease and the conversion degree increases to values close to the final value depending on the curing temperature (0.75 for T_c=50°C, or 0.92 for T_c=80°C). The kinetics of this second step is clearly slower than in the former as a consequence of the consumption of reactive groups and to the increase of the overall degree of conversion. For a di-functional epoxy and a hexa-functional amine hardener which react in ideal conditions, the gel point is achieved at α_{gel}=0.45. Taking into account the values of conversion of this second step, one may consider that the reaction occurs practically in the gel phase.

Table 1
Glass transition temperature of the fully cured epoxy-triamine resin

	q_0 (°C min^{-1})	T_{g_0} (°C)	$T_{g_{mp}}$ (°C)	T_{g_e} (°C)	Averaged scans[a]
DSC	10	81.6±0.9	85.8±0.7	89.7±0.6	11
ADSC, $|C_p^*|$	1	81.1±0.7	85.8±0.5	90.0±0.6	9
ADSC, $|C_p^*|$	−1	90.8±0.7	85.5±0.7	79.9±0.9	6
ADSC, HF reversing	1	81.1±0.6	85.8±0.6	89.9±0.7	6
ADSC, HF total	1	78±1	82.3±0.8	86.5±0.7	7

ADSC: modulation: 0.5°C and 1 min.

[a] Number of scans averaged to obtain the indicated value of T_g.

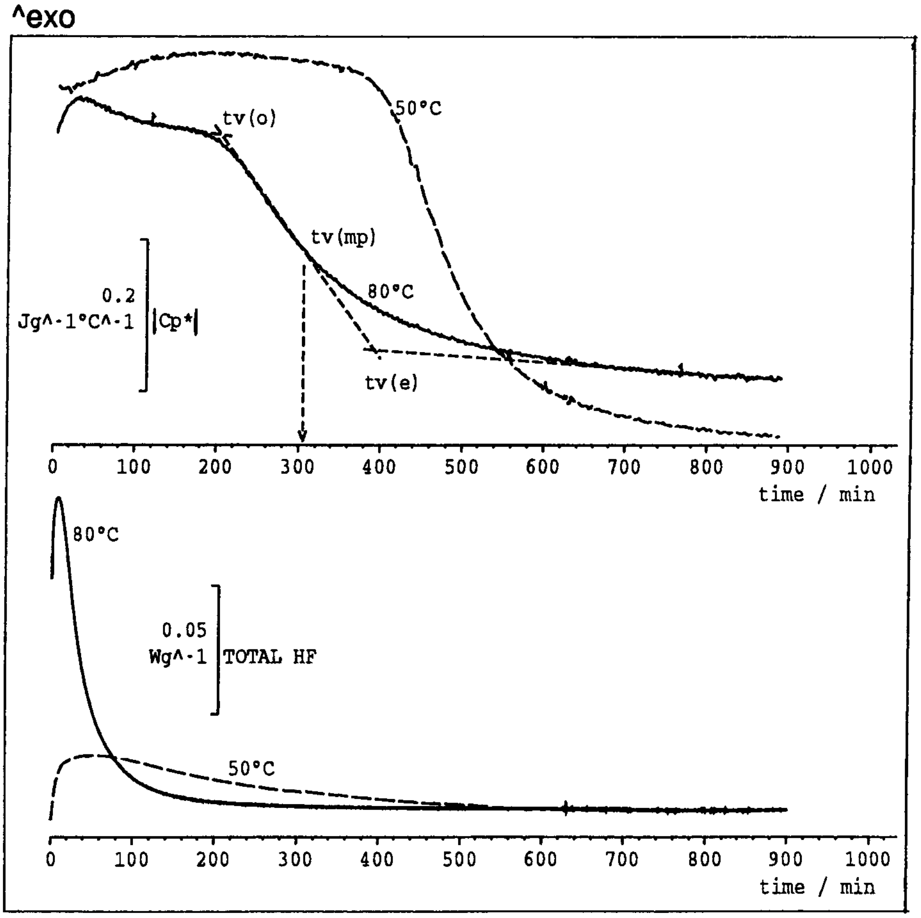

Fig. 3. Total heat flow and modulus of the complex specific heat capacity for the quasi-isothermal curing of the epoxy-triamine system at 50°C and 80°C, with 0.5 K and 1 min modulation. $|C_p^*|$ curve at 80°C indicates the determination of the extrapolated onset $t_{v(o)}$, midpoint $t_{v(mp)}$, and extrapolated endset $t_{v(e)}$ vitrification times.

The initial increase in $|C_p^*|$ may be attributed to the formation of the linear and crosslinked structure by reaction of the primary amine with the epoxy groups. According to Cassettari et al. [5] this reaction implies an increase in the configurational entropy or number of configurational states of the system, and subsequently an increase of the heat capacity. At the same time, the secondary amine groups react with a lower rate constant [15–17] giving the tertiary amine structure. In this reaction we may expect a decrease of the number of configurational states in the tertiary amine structure resulting the small decrease in $|C_p^*|$. These results are in agreement with those of Van Mele and co-workers obtained in the cure of DGEBA by methylene dianiline (Fig. 12 in [18]). The authors estimate the changes in heat capacity which allow to distinguish between primary and secondary amine-epoxy reactions. Other results obtained in DGEBA cured by ethylene diamine (Figs. 2 and 5 in [5]) and a tetra-

Table 2
Time, conversion and shape of the maximum in $|C_p^*|$

T_c (°C)	$t_{\max|C_p^*|}$ (min)	α ($t_{\max}$)	Shape
50	150–190	0.49–0.56	Very broad
60	75–105	0.42–0.53	Very broad
70	40	0.43	Broad
80	30	0.54	Peak
85	19	0.44	Peak
90	13	0.43	Peak

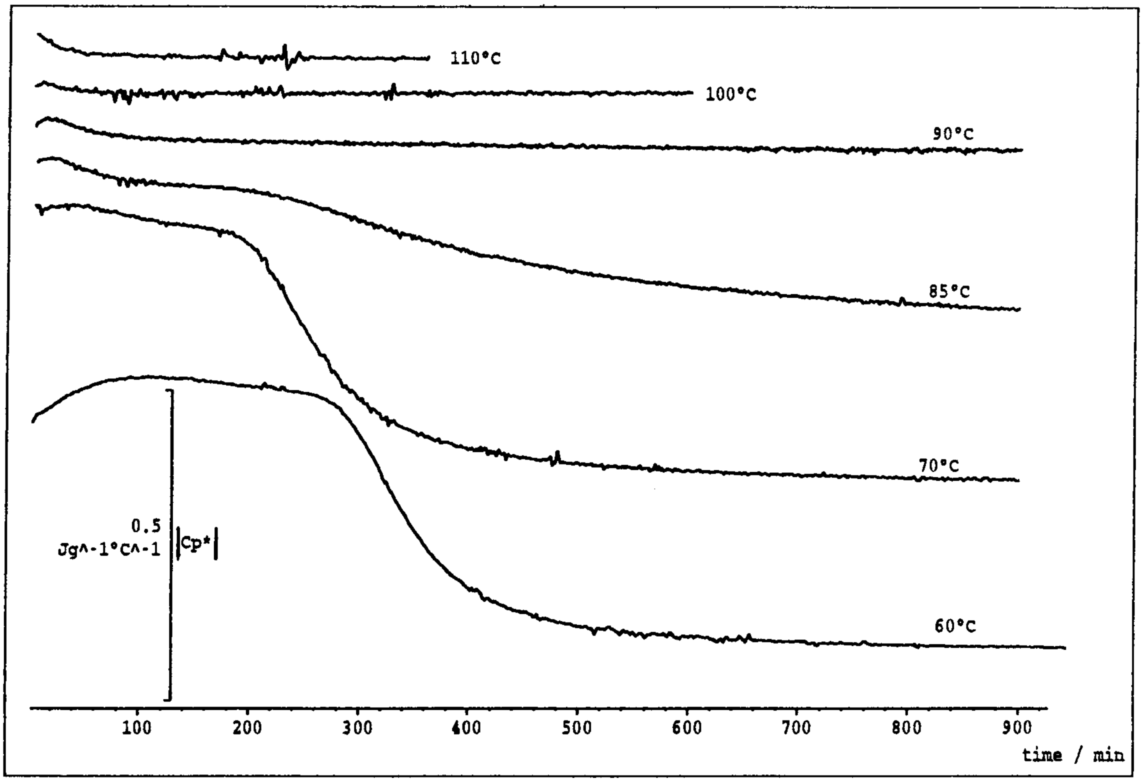

Fig. 4. Modulus of the complex specific heat capacity for the quasi-isothermal curing of the epoxy-triamine system at 60°C, 70°C, 85°C, 90°C, 100°C and 110°C, with 0.5 K and 1 min modulation.

functional epoxy cured by a tetra-functional amine (Fig. 2 in [6]) show only the increase in heat capacity, the maximum of which occurs close to the maximum in the heat flow trace.

The following step is characterised by a dramatic decrease of the complex heat capacity, ΔC_p^*, corresponding to a small increase of the conversion degree depending inversely on the proximity to the glass transition region (at T_c=50°C, the conversion changes from 0.75 to 0.82, and at T_c=80°C changes from 0.92 to 0.93). This decay in $|C_p^*|$ is also shown at 85°C, although less abruptly than at 80°C, but it is not observed for $T_c \geq 90$°C, above T_{g_∞}, as Fig. 4 shows. This effect indicates that this decrease in $|C_p^*|$ is related to the vitrification of the system. This result agrees with that obtained by other authors [5–7,18]. In this step, an empirical vitrification time $t_{v(mp)}$ may be defined as the midpoint of the ΔC_p^* decay. The values of the vitrification time at the midpoint ($t_{v(mp)}$), and in the extrapolated onset ($t_{v(o)}$) and endset ($t_{v(e)}$) points are shown in the Table 3.

The vitrification time may be also determined by conventional DSC using the so-called method of partial curing, where the samples are cured separately at different times, and submitted to a DSC analysis in order to determine the glass transition and the extent of cure. Using this technique, the vitrification time, t_v, is empirically determined as the point where the T_g equals to T_c (Fig. 5). As Table 3 shows, the values obtained for t_v by the method of partial curing agree well with those obtained by the variation in $|C_p^*|$.

It is interesting to observe that the decay in $|C_p^*|$ occurs at longer times than the decrease observed in the total heat flow, after the peak. In the epoxy-amine systems studied in [5,6], the decay in the heat capacity was observed at practically the same time as the decrease in the heat flow. This different behaviour may be a consequence of the presence of the polyoxypropylene chains in the crosslinks which are able

Table 3
Vitrification properties (time and conversion degree) determined by ADSC from complex heat capacity, total heat flow, phase angle and by conventional DSC (partial curing method) (see text for terminology)

T_c (°C)	$\lvert C_p^*\rvert$				HF_{total}	δ	C_p'' (J g^{-1} K^{-1})	DSC (partial curing)	
	$t_{v(o)}$ (min)	$t_{v(mp)}$ (min)	$t_{v(e)}$ (min)	ΔC_p^* (J g^{-1} K^{-1})	α ($t_{v(mp)}$)	$t_{v(\delta)}$ (min)	$t_{v(C_p'')}$ (min)	t_v (min)	α (t_v)
50	392	472	552	0.45	0.80	450	435	427	0.80
60	280	339	398	0.38	0.82	320	315	310	0.85
70	199	259	320	0.36	0.86	240	235	265	0.90
80	207	307	395	0.29	0.93	270	255	300	0.95
85	210	380	495	0.15	0.96	–	–	–	–

to give greater chain segmental mobility and shifts the vitrification to longer times and to higher conversion values than in model systems such as DGEBA–ethylene diamine resins [5].

The decay in $|C_p^*|$ during the vitrification is a consequence of a restriction in the mobility of the reactive centres; the system reaches the glassy state and in these conditions the reaction becomes controlled by diffusion. Consequently, the kinetics slow down and the extent of conversion tends to a constant value [2–4,19–23]. Moreover, as the system has reached the glassy state, the slow segmental motions caused by the structural relaxation of the glass may determine the control of the reaction rate [3,4].

After this abrupt decay, $|C_p^*|$ changes very slowly and becomes nearly constant. This tendency has been observed at 60°C for curing times longer than 900 min (which results are not shown in Figs. 3 and 4). This behaviour agrees with the prediction of the Hutchinson–Montserrat theoretical model of enthalpy relaxation by TMDSC [12]. When the vitrification of the resin is completed, the conversion degree remains practically constant and the system experiments a physical ageing process at T_c. According to the cited model, $|C_p^*|$ should remain constant during the physical ageing [24], while the total heat flow will decrease due to the endothermic nature of the process (at the moment the heat flow evolved during physical ageing cannot be detected by the present calorimeters).

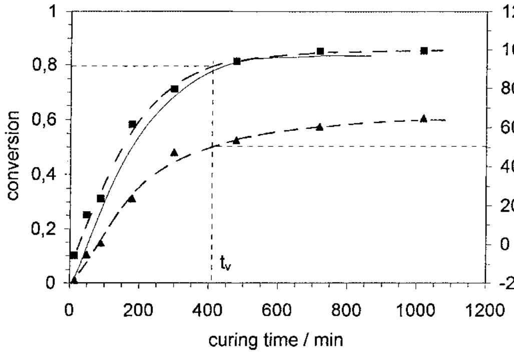

Fig. 5. Variation of the conversion (■) and the glass transition, T_g, (▲) for the isothermal curing of the epoxy-triamine resin at 50°C, obtained by the partial curing method using conventional DSC; t_v is the vitrification time obtained when T_g=T_c. The solid line corresponds to the conversion calculated from ADSC total heat flow. The dashed lines are a guide for the eye.

The phase angle δ, and the out-of-phase heat capacity C_p'' show an asymmetric wide peak in this region (Figs. 6 and 7, respectively). When the reacting system changes from a viscous liquid to a glassy polymer there is a relaxation process and the phase angle between the temperature modulation and the heat flow changes. In both properties, δ and C_p'', a vitrification time corresponding to the peak may be determined, $t_{v(\delta)}$ and $t_{v(C_p'')}$. Both vitrification times take place at lower values than the $t_{v(mp)}$ determined by ΔC_p^* as is shown in Table 3. At $T_c \geq 90$°C, both the phase angle and C_p'' show an initial decrease and subsequent constancy is observed.

4.3. Variation of heat capacity during the vitrification process

A variation of the modulus of the complex heat capacity, ΔC_p^*, during the vitrification may be empiri-

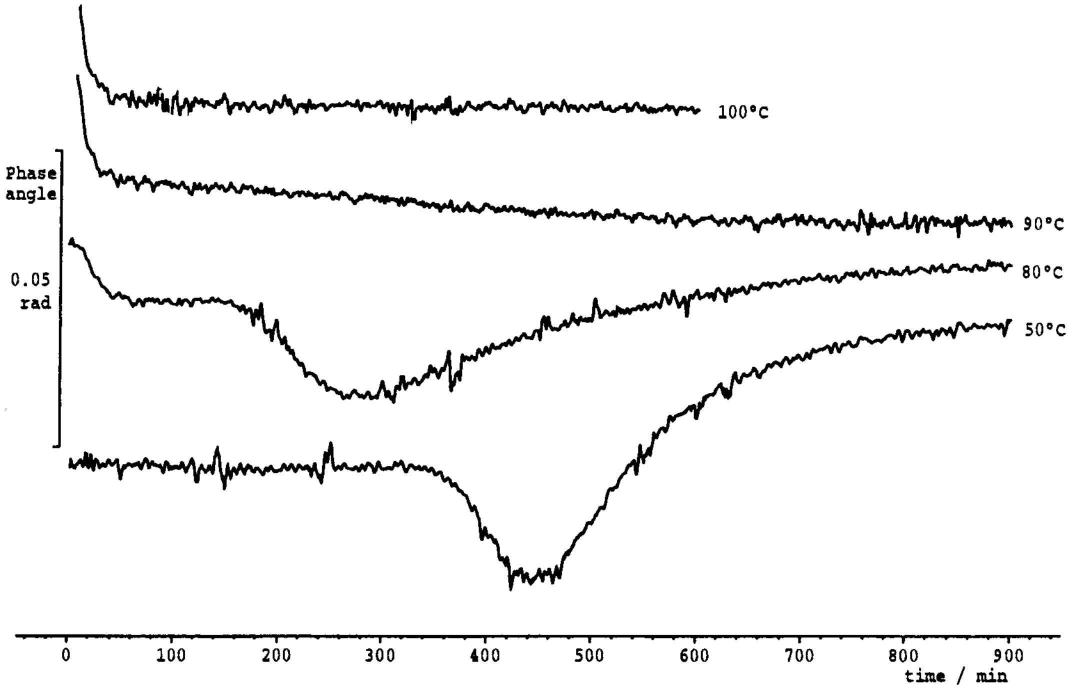

Fig. 6. Phase angle in radians for the quasi-isothermal curing of the epoxy-triamine system at 50°C, 80°C, 90°C and 100°C with 0.5 K and 1 min modulation.

cally defined as

$$\Delta C_p^* = |C_p^*|(t_{\mathrm{v(e)}}) - |C_p^*|(t_{\mathrm{v(o)}}), \tag{9}$$

where $|C_p^*|(t_{\mathrm{v(o)}})$ and $|C_p^*|(t_{\mathrm{v(e)}})$ are the values of $|C_p^*|$ at the extrapolated onset and endset points, respectively. It is observed that ΔC_p^* decreases with increasing curing temperature (Table 3). Between 50 and 80°C, a linear relationship between ΔC_p^* and $1/T_c$ is observed (Fig. 8):

$$\Delta C_p^* = -1.645 + \frac{679.7}{T_c} \quad (\mathrm{J\,g^{-1}\,K^{-1}}) \tag{10}$$

with a regression coefficient of r^2=0.963. This interval of ΔC_p^* corresponds to the vitrification process of the system, then the curing temperature is equal to the T_g and the equation has the same dependence to that proposed by Boyer [25] in the glass transition region: $\Delta Cp(T_g)=a+(b/T_g)$. In an epoxy system, a decrease in $\Delta Cp(T_g)$ has been observed when the degree of cross-linking or the T_g increases [26].

The relation between ΔC_p^* and T_c, which is the T_g of the system at vitrification, may be understood in terms of the Gibbs–DiMarzio theory of the glass transition [27], that predicts an increase in T_g with the chain stiffness. On the other hand, stiffness is supposed to decrease the configurational entropy, and subsequently to decrease the variation between the heat capacity of the liquid-like and the glassy states.

From Figs. 3 and 4 it is also observed that the interval of vitrification time, measured as the difference between the endset and onset times, tends to increase when the temperature approaches T_{g_∞}.

4.4. Mobility factor during diffusion controlled process

The decay in $|C_p^*|$ during vitrification may be normalised between unity and zero [6,7] by a mobility factor, MF:

$$\mathrm{MF} = \frac{|C_p^*|(t,T) - |C_{p,\mathrm{g}}^*|(T)}{|C_{p,\mathrm{l}}^*|(t_0,T) - |C_{p,\mathrm{g}}^*|(T)}, \tag{11}$$

where MF=1 is assigned up to the onset of the vitrification decay when $|C_p^*|(t,T) = |C_{p,\mathrm{l}}^*|(t_0,T)$,

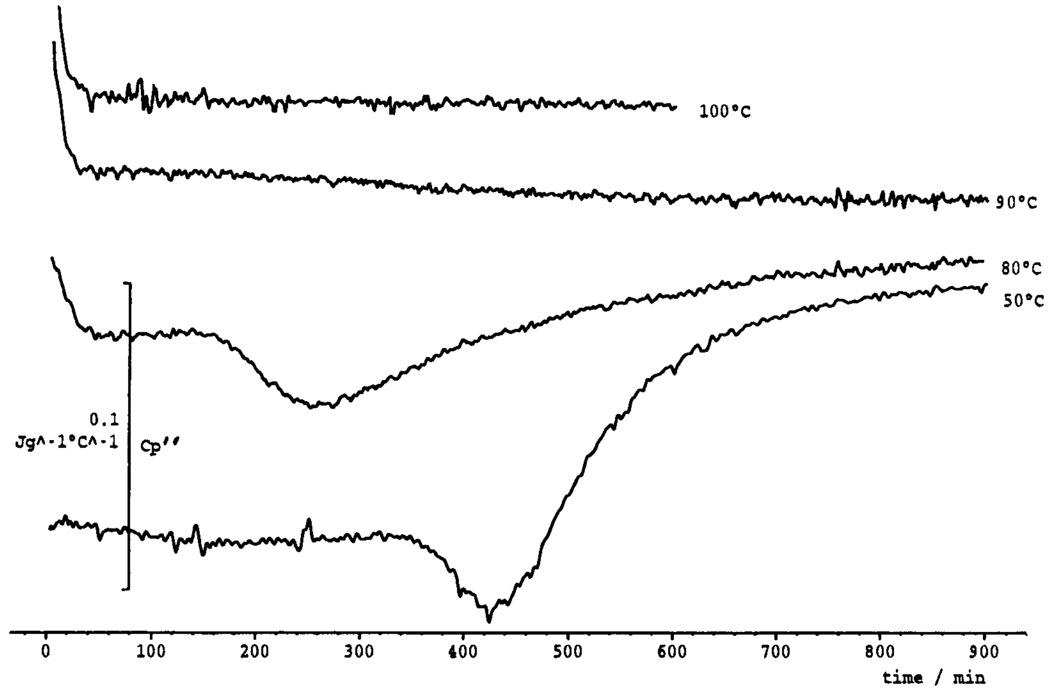

Fig. 7. Out-of-phase heat capacity in J g^{-1} K^{-1} for the quasi-isothermal curing of the epoxy-triamine system at 50°C, 80°C, 90°C, 100°C with 0.5 K and 1 min modulation.

and MF=0 is assigned to the end of the vitrification at $|C^*_{p,g}|(T)$. In our epoxy system, the constancy in $|C^*_p|$ in the glassy state was not fully obtained ever after 900 min of reaction. However, its variation was very small, and consequently we take a value at around 900–1000 min for $|C^*_{p,g}|(T)$.

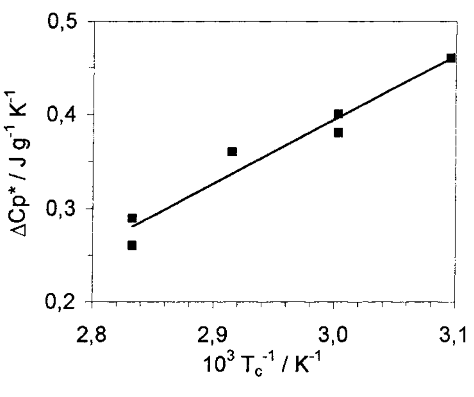

Fig. 8. Dependence of the variation of $|C^*_p|$ at vitrification on the reciprocal of the curing temperature in the range between 50°C and 80°C. The line corresponds to a linear regression which parameters are shown in Eq. (10).

The mobility factors for curing temperatures between 50°C and 85°C are shown in Fig. 9. A sigmoidal shape is observed, which allows to determine an inflexional slope:

$$\hat{s} = -\left[\frac{\mathrm{d(MF)}}{\mathrm{d}t}\right]_{\mathrm{inf}}. \qquad (12)$$

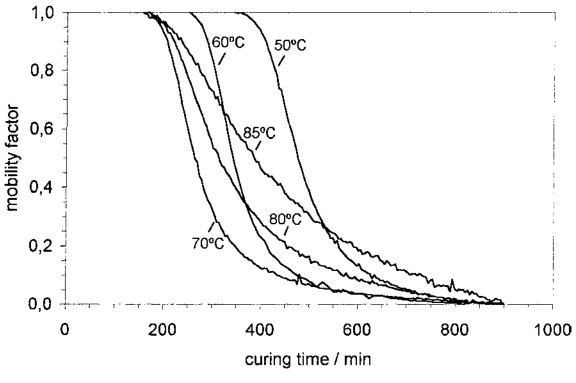

Fig. 9. Variation of the mobility factor, MF, with the curing time for the indicated curing temperatures. The values of MF were calculated by Eq. (11).

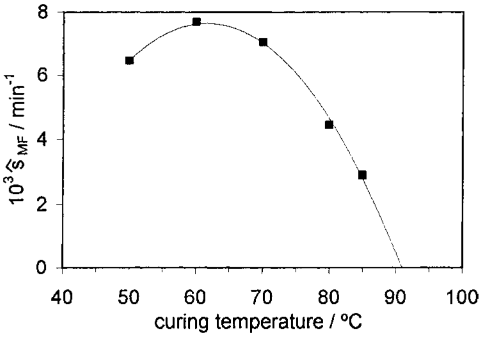

Fig. 10. Dependence of the inflexional slope of the mobility factor on the curing temperature. The line corresponds to a second order polynomial regression.

It is observed that this inflexional slope tends to decrease when T_c approaches T_{g_∞} (Fig. 10), extrapolating to zero at approximately 90°C. The endset value of the glass transition region in the fully cured epoxy resin is about 90°C, so that this result agrees with the fact that no vitrification effects are observed when the curing is performed above the T_g interval. As the rapid decay in $|C_p^*|$ is a consequence of the vitrification process, the inflexional slope is an average measure of the rate of vitrification of the system.

According to Van Mele et al. [28], the mobility factor gives us a criterion to plot the vitrification line in a temperature-time-transformation (TTT) diagram. Fig. 11 shows in a TTT diagram different isomobility lines for mobility factors from 1 to less than 0.05. The line at MF=0.5 may be considered the vitrification line. The values of vitrification time for this mobility factor are practically the same as those determined from the midpoint of the decay in $|C_p^*|$. Isomobility lines between 1 and 0.9 may characterise the beginning of the vitrification process, and the line for MF<0.05 indicates that the system may be considered in the glassy state.

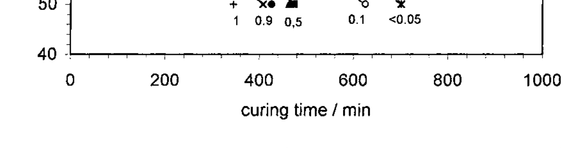

Fig. 11. Temperature–time-transformation diagram showing different isomobility lines. The solid line shows the vitrification line obtained by the points where MF=0.5 (■). The vitrification times obtained by ΔC_p^* (▲), and by the partial curing method (●) are also shown. The lines are a guide for the eye.

4.5. Kinetics of the curing reaction

As was mentioned in Section 1, the rate of cure is controlled by the mobility of the reacting centres and their chemical reactivity. In the first stages of the curing, the rate is controlled by the chemical kinetics. When the degree of crosslinking increases, the mobility of the groups is reduced and the control by chemical reaction is accompanied by the control by diffusion. With vitrification, the system passes to the glassy state and the rate is mainly diffusion controlled [2]. In order to study the diffusion control stage, many approaches have been proposed which have been reviewed by Mita and Horie [23] and by Wise et al. [22]. One fundamental approach considers that the overall rate of cure is composed of two components, one associated with the chemical reaction step and the other with the diffusion reaction step [2,20,22,29]. Other authors use empirical expressions based on the reduction of the free volume during curing to model the effect of diffusion control [21,30]. Using modulated DSC, Van Mele et al. [6,7] proposed an empirical model based on a normalised diffussion factor in order to describe the effects of the decrease of the mobility on the reaction rate:

$$\left[\frac{\mathrm{d}\alpha}{\mathrm{d}t}(\alpha,T)\right]_{\mathrm{obs}} = \left[\frac{\mathrm{d}\alpha}{\mathrm{d}t}(\alpha,T)\right]_{\mathrm{kin}} \cdot \mathrm{DF}(\alpha,T), \tag{13}$$

where α is the conversion, $(\mathrm{d}\alpha/\mathrm{d}t)_{\mathrm{obs}}$ is the experimentally observed reaction rate, and $(\mathrm{d}\alpha/\mathrm{d}t)_{\mathrm{kin}}$ is the chemical rate calculated by a model for the chemical kinetics in the absence of diffusion control. DF(α,T) is a normalised diffusion factor correcting the chemical rate in conditions of restricted mobility. This factor ranges from unity in the unrestricted state, to zero in the frozen glass. These authors [6,7] show that for the epoxy systems this diffusion factor coincides with the mobility factor calculated from the complex heat capacity measurements. In other words, MF can be used as a direct measurement of the decrease of the reaction rate due to the mobility restrictions in the diffusion control regime [6,7]. Then, in order to simulate the reaction rate of the curing process the following equation may be used:

$$\left[\frac{\mathrm{d}\alpha}{\mathrm{d}t}(\alpha, T)\right]_{\mathrm{obs}} = \left[\frac{\mathrm{d}\alpha}{\mathrm{d}t}(\alpha, T)\right]_{\mathrm{kin}} \cdot \mathrm{MF}(\alpha, T), \tag{14}$$

where $(\mathrm{d}\alpha/\mathrm{d}t)_{\mathrm{kin}}$ is the chemical reaction rate modelled by an empirical equation, and MF is the mobility factor calculated by Eq. (11). The chemical reaction rate may be calculated by the autocatalytic model (Sesták–Berggren model) as indicated elsewhere [31]:

$$\left[\frac{\mathrm{d}\alpha}{\mathrm{d}t}(\alpha, T)\right]_{\mathrm{kin}} = k.\alpha^m(1-\alpha)^n, \tag{15}$$

where k is a rate constant of Arrhenium type:

$$k = A.\mathrm{e}^{-E/RT}, \tag{16}$$

E being the activation energy. The kinetic parameters were calculated by the method proposed by Málek [32], which has also been applied to other epoxy systems [31,33]. The activation energy E was first calculated by the isoconversional method from ADSC heat flow traces from conversions between 0.3 and 0.5, and curing temperatures from 50°C to 90°C. The slope of $\ln t$ against $1/T_c$ at different conversions give the value of the activation energy [33]. An average value of 57.5 kJ mol^{-1} was calculated. Table 4 shows the kinetic parameters m, n and $\ln A$ obtained by multilinear regression of ADSC heat flow data using Eqs. (15) and (16).

Fig. 12 shows the experimental reaction rate at 50°C, $(\mathrm{d}\alpha/\mathrm{d}t)_{\mathrm{obs}}$, calculated from the ADSC heat flow data, the reaction rate calculated from kinetic Eq. (15), $(\mathrm{d}\alpha/\mathrm{d}t)_{\mathrm{kin}}$, and the reaction rate simulated using the mobility factor and applying Eq. (14), $(\mathrm{d}\alpha/\mathrm{d}t)_{\mathrm{calc}}$. The results show a very good agreement between the experimental and the simulated rate. A similar agreement was found at 60°C, 70°C and 80°C.

Table 4
Kinetic parameters obtained by ADSC heat flow data and constant value of activation energy of 57.5 kJ mol^{-1}

T_c (°C)	m	n	$\ln A$
50	0.24	1.48	12.3
60	0.23	1.61	12.2
80	0.23	1.61	12.3
90	0.18	1.86	12.3
100	0.08	2.23	12.0

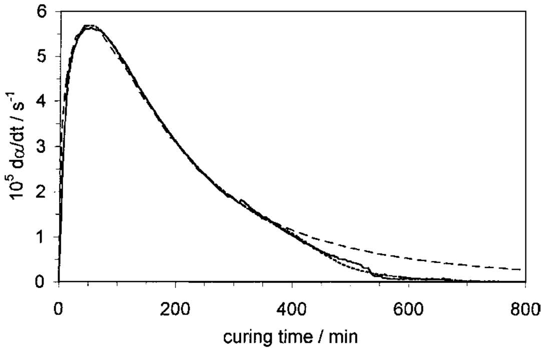

Fig. 12. Rate of conversion against curing time for the curing at 50°C. The solid line shows the experimental reaction rate $(\mathrm{d}\alpha/\mathrm{d}t)_{\mathrm{obs}}$. The dashed lined (- - -) corresponds to the kinetic rate, $(\mathrm{d}\alpha/\mathrm{d}t)_{\mathrm{kin}}$, obtained by Eq. (15), without mobility restrictions. The simulated rate obtained by the product of the kinetic rate and the mobility factor is also shown (· · ·).

5. Conclusions

The quasi-isothermal curing of an epoxy-triamine system has been studied by alternating differential scanning calorimetry (ADSC), which is a temperature modulated differential scanning calorimetry (TMDSC) technique. This technique allows the study of the kinetics of the curing reaction when it is controlled mainly by the chemical reactivity of the functional groups and also when it is controlled by the diffusion of the reactive centres, as is the case for low curing temperatures ($T_c < T_{g_\infty}$).

In this epoxy-triamine system, the complex heat capacity shows a variation in three steps. Initially, $|C_p^*|$ increases until a peak is reached, followed by a slight decrease. This peak becomes sharper and shifts to lower curing times as T_c increases. The kinetics in the second step is slower than in the first, which is related mainly to the lower constant rate for the secondary amine hydrogen reaction.

During vitrification, an abrupt decay of $|C_p^*|$ is observed which allows the determination of an empirical vitrification time at the midpoint of ΔC_p^*. This value agrees with that obtained by the partial curing method. The phase angle and the out-of-phase heat capacity show an asymmetric wide peak in this region. The peak temperature gives a value of the vitrification time which is very close to that obtained by ΔC_p^*. The change in $|C_p^*|$ at vitrification decreases with T_c.

As a consequence of the vitrification, the reaction becomes diffusion controlled and the degree of conversion tends to a practically constant value. Following vitrification, $|C_p^*|$ changes very slowly and tends to be constant as does the conversion.

The decay in $|C_p^*|$ during vitrification may be normalised between unity and zero by introducing a mobility factor, MF. The inflexional slope of the mobility factor is an average measure of the rate of vitrification of the system. The times at MF=0.5 agree with the vitrification times calculated by the midpoint in ΔC_p^*. Additionally this mobility factor allows to simulate the kinetics during the stage where the reaction is diffusion controlled. The observed reaction rate may be simulated by the product of the kinetic reaction rate and the mobility factor.

Acknowledgements

Financial support has been provided by CICYT Project no. MAT 97-0634-C02-02. The authors are grateful to CIBA-GEIGY and Hunstman Corporation for supplying the materials, and to Dr. J.M. Hutchinson whose comments and discussion of the manuscript were very helpful.

References

[1] B. Ellis, The Kinetics of cure and network formation, in: B. Ellis (Ed.), Chemistry and Technology of Epoxy Resins, Chapter 3, Blakie, London, 1993.

[2] I. Havlícek, K. Dusek, in: B. Sedlácek, J. Kahovec (Eds.), Crosslinked Epoxies, Walter de Gruyter, Berlin, 1987, pp. 417–424.

[3] J.K. Gillham, Polym. Eng. Sci. 26 (1986) 1429.

[4] S. Montserrat, J. Appl. Polym. Sci. 42 (1992) 545.

[5] M. Cassettari, G. Salvetti, E. Tombari, S. Veronesi, G.P. Johari, J. Polym. Sci. Polym. Phys. 31 (1993) 199.

[6] G. Van Assche, A. Van Hemelrijck, H. Rahier, B. Van Mele, Thermochim. Acta 268 (1995) 121.

[7] G. Van Assche, A. Van Hemelrijck, H. Rahier, B. Van Mele, Thermochim. Acta 304–305 (1997) 317.

[8] M. Reading, D. Elliot, V.L. Hill, Proceedings of the 21st NATHAS, 1992, p. 145.

[9] M. Reading, D. Elliot, V.L. Hill, J. Therm. Anal. 40 (1993) 949.

[10] S. Gill, S.R. Sauerbrunn, M. Reading, J. Therm. Anal. 40 (1993) 931.

[11] A. Boller, Ch. Schick, B. Wunderlich, Thermochim. Acta 266 (1995) 97.

[12] J.M. Hutchinson, S. Montserrat, Thermochim. Acta 304–305 (1997) 257.

[13] J. Schawe, Thermochim. Acta 261 (1995) 183.

[14] R.B. Prime, in: E.A. Turi (Ed.), Thermal Characterization of Polymeric Materials, vol. 2, Chapter 6, Academic Press, New York, 1997.

[15] D. Verchere, H. Sauterau, J.P. Pascault, C.C. Riccardi, S.M. Moschiar, R.J.J. Willams, Macromolecules 23 (1990) 725.

[16] S. Paz-Abuin, M. Pazos Pellin, M. Paz-Pazos, A. López-Quintela, Polymer 38 (1997) 3785.

[17] B.A. Rozenberg, Adv. Polym. Sci. 75 (1985) 113.

[18] S. Swier, G. Van Assche, A. Van Hemelrijck, H. Rahier, E. Verdonck, B. Van Mele, J. Therm. Anal. 54 (1998) 585.

[19] H.E. Bair, Polym. Preprints 26 (1985) 10.

[20] G. Wisanrakkit, J.K. Gillham, J. Coatings Tech. 62 (1990) 35.

[21] H. Stutz, J. Mertes, K. Neubecker, J. Polym. Sci. Polym. Chem. 31 (1993) 1879.

[22] C.W. Wise, W.D. Cook, A.A. Goodwin, Polymer 38 (1997) 3251.

[23] I. Mita, K. Horie, J. Macromol. Sci. Rev. Macromol. Chem. Phys. C 27 (1987) 91.

[24] J.M. Hutchinson, personal communication.

[25] R.F. Boyer, J. Macromol. Sci. Phys. B 7 (1973) 487.

[26] S. Montserrat, Polym. Commun. 36 (1995) 435.

[27] J.H. Gibbs, E.A. DiMarzio, J. Chem. Phys. 28 (1958) 373.

[28] A. Van Hemreljick, B. Van Mele, J. Therm. Anal. 49 (1997) 437.

[29] E. Rabinovitch, Trans. Faraday Soc. 33 (1937) 1225.

[30] C.S. Chern, G.W. Poehlein, Polym. Eng. Sci 27 (1987) 788.

[31] S. Montserrat, J. Málek, Thermochim. Acta 228 (1993) 47.

[32] J. Málek, Thermochim. Acta 200 (1992) 257.

[33] S. Montserrat, G. Andreu, P. Cortés, Y. Calventus, P. Colomer, J.M. Hutchinson, J. Málek, J. Appl. Polym. Sci. 61 (1996) 1663.